Drug Design, Development and Therapy

Dovepress
open access to scientific and medical research

Open Access Full Text Article

ORIGINAL RESEARCH

NMMHC IIA Inhibition Ameliorates Cerebral Ischemic/Reperfusion-Induced Neuronal Apoptosis Through Caspase-3/ROCK1/MLC Pathway

This article was published in the following Dove Press journal:
Drug Design, Development and Therapy

Guang-Yun Wang[1]
Tie-Zheng Wang[1]
Yuan-Yuan Zhang[1]
Fang Li[1]
Bo-Yang Yu[2]
Jun-Ping Kou[1]

[1]State Key Laboratory of Natural Products, Jiangsu Key Laboratory of TCM Evaluation and Translational Research, Department of Pharmacology of Chinese Material Medica, School of Traditional Chinese Pharmacy, China Pharmaceutical University, Nanjing 211198, People's Republic of China; [2]State Key Laboratory of Natural Products, Jiangsu Key Laboratory of TCM Evaluation and Translational Research, Department of Resource and Development of Chinese Material Medica, School of Traditional Chinese Pharmacy, China Pharmaceutical University, Nanjing 211198, People's Republic of China

Purpose: Our previous studies have indicated that non-muscle myosin heavy chain IIA (NMMHC IIA) is involved in H_2O_2-induced neuronal apoptosis, which is associated with the positive feedback loop of caspase-3/ROCK1/MLC pathway. However, the neuroprotective effect of NMMHC IIA inhibition with an adeno-associated virus (AAV) vector after transient middle cerebral artery occlusion (MCAO) and its role in caspases-3/ROCK1/MLC pathway remain blurred.

Methods: Green fluorescent protein (GFP) and a small hairpin RNA targeting Myh9 (encoding NMMHC IIA) were cloned and packaged into the AAV9 vector. AAV-shMyh9 or control vector were injected into C57BL/6J mice four weeks prior to 60 min MCAO. Twenty-four hours after reperfusion, functional and histological analyses of the mice were performed.

Results: In this study, AAV-shMyh9 was used to down-regulate NMMHC IIA expression in mice. We found that down-regulation of NMMHC IIA could improve neurological scores and histological injury in ischemic mice. Ischemic attack also activated neuronal apoptosis, and this effect was partially attenuated when NMMHC IIA was inhibited by AAV-shMyh9. In addition, AAV-shMyh9 significantly reduced cerebral ischemic/reperfusion (I/R)-induced NMMHC IIA-actin interaction, caspase-3 cleavage, Rho-associated kinase1 (ROCK1) activation and myosin light-chains (MLC) phosphorylation.

Conclusion: Consequently, we showed that AAV-shMyh9 inhibits I/R-induced neuronal apoptosis linked with caspase-3/ROCK1/MLC/NMMHC IIA-actin cascade, which has also been confirmed to be a positive feedback loop. These findings put some insights into the neuroprotective effect of AAV-shMyh9 associated with the regulation of NMMHC IIA-related pathway under ischemic attack and provide a therapeutic strategy for ischemic stroke.

Keywords: NMMHC IIA, adeno-associated virus, ischemic stroke, apoptosis

Introduction

Ischemic stroke is one of the main causes of death and disability worldwide, which is due to decreased cerebral blood flow and insufficient cerebral oxygen supply.[1,2] Although we have made great breakthroughs in understanding the pathophysiology of ischemic stroke, there is no effective and safe treatment at present. Thrombolytic therapy is the most effective treatment in clinic, but its limited time window and the associated high recurrence rate limit its clinical application.[3,4] Therefore, there is an extremely urgent need to find new and effective therapeutic targets and drugs for ischemic stroke.

Apoptosis is one of the main forms of neuronal death induced by ischemic stroke, which has been extensively studied.[5–7] By now, it has been shown that Bcl-2, Bax, caspase-3, and p53 are important proteins in the apoptotic cascade reaction.

Correspondence: Jun-Ping Kou
State Key Laboratory of Natural Products, Jiangsu Key Laboratory of TCM Evaluation and Translational Research, Department of Pharmacology of Chinese Material Medica, School of Traditional Chinese Pharmacy, China Pharmaceutical University, Nanjing 211198, People's Republic of China
Email junpingkou@cpu.edu.cn

submit your manuscript | www.dovepress.com
DovePress
http://doi.org/10.2147/DDDT.S230882

Knockout both caspase-3 and p53 decreased ischemic injury, and a similar result is observed for Bcl-2 overexpression.[8] Rho-associated kinase1 (ROCK1) is a Rho-binding protein with serine/threonine protein kinase activity, which is closely related to the process of apoptosis and cell membrane blebbing. ROCK1 is a direct substrate of caspase-3 and is activated by caspase-3-mediated cleavage at its C-terminus inhibitory region. ROCK1 can also directly induce phosphorylation of myosin light-chains (MLC).[9,10] We have previously illustrated the caspase-3/ROCK1/MLC feedback loop in hydrogen peroxide (H_2O_2)-induced PC12 cell apoptosis, and the non-muscle myosin heavy chain IIA (NMMHC IIA)-actin interaction regulates caspase-3/ROCK1/MLC signal cascade by a feedback mechanism upon oxidative stress-induced neuronal apoptosis.[11,12] NMMHC IIA, a member of the cytoskeleton, which is encoded by myosin heavy 9 (Myh9) gene and interacts with actin filaments to form a contractile unit.[13–15] Additionally, NMMHC IIA has been identified to participate in blood-brain barrier (BBB) dysfunction in ischemia stroke,[16] and the NMMHC IIA-actin interaction mediates oxidative stress-induced neuronal apoptosis.[12] However, the correlation between NMMHC IIA and the caspase-3/ROCK1/MLC positive feedback loop in ischemic stroke remains unknown. Moreover, it is also not clear whether breaking the positive feedback loop by interfering with NMMHC IIA can improve cerebral ischemic injury.

In order to further study the above problems, we specific knockdown NMMHC IIA by intravenous injection of adeno-associated virus (AAV) vector (AAV-shMyh9). Among the many virus vector systems, AAV is now widely used to deliver genes to the central nervous system (CNS) due to its safety and efficacy, both as research tools and in clinical studies.[17–20] AAV-mediated gene delivery before the ischemic attack has also been used to assess the neuroprotective effect of vector-encoded proteins in cerebral ischemia.[21,22]

In the present study, we established a mice transient middle cerebral artery occlusion (MCAO/R) model to investigate the role of NMMHC IIA inhibition mediated by RNAi in apoptosis and underlying regulatory mechanism. We found that AAV-shMyh9 could attenuate neuronal apoptosis, which is related to inhibiting NMMHC IIA-actin interaction and caspase-3/ROCK1/MLC signaling pathway. It provides the correlation between NMMHC IIA and the caspase-3/ROCK1/MLC positive feedback loop in ischemic stroke and provides empirical evidence for targeting it in the clinical treatment of cerebral ischemia.

Materials and Methods

Animals and Treatment

Male specified-pathogen-free (SPF) C57BL/6J mice weighing 18–22 g were obtained from the Reference Animal Research Centre of Yangzhou University (Yangzhou, China; certificate no SCXK 2017–0001). All experimental protocols were performed according to the National Institutes of Health (NIH) guidelines, and the research was approved by the Institutional Animal Care and Use Committee of the Animal Ethics Committee of the School of Chinese Materia Medica, China Pharmaceutical University. In our experiment, the 60 mice were divided randomly into four groups (n=15 in each group): sham operated (Sham), Sham+AAV9-shMyh9-GFP, I/R, and the I/R+AAV9-shMyh9-GFP groups. The Sham group and I/R group were administered AAV9-control-GFP.

rAAV Vectors and Infection

To knockdown NMMHC IIA expression, three chains of mouse rAAV-shMyh9-GFP were generated by Vigene Bioscience (Rockville, MD, USA). The one that resulted in the most significant down-regulation of endogenous NMMHC IIA expression was selected for further experiments. rAAV vectors were diluted in phosphate-buffered saline (PBS) to 3×10^{11} genome copies/100 μL before administration. rAAV vectors were injected intravenously into male C57BL/6J mice via the mouse tail vein with an AAV9-control-GFP or AAV9-shMyh9-GFP (1.5×10^{11} genome copies/mouse). After four weeks of injection, cerebral ischemia/reperfusion (I/R) can be performed, and then other experiments could be carried out.

MCAO/R Procedures

The MCAO/R model was prepared in mice as described previously.[23] Cerebral ischemia was induced by intraluminal occlusion of the right middle cerebral artery using a silicone rubber-coated 6–0 nylon monofilament. To confirm the cerebral artery blood flow, a laser Doppler flow meter (LDF; FLPI2, Moor, UK) was used. Approximately 1 h after occlusion, the suture was withdrawn to allow reperfusion for 24 h. Neurological deficit was examined using Longa's method.[23] Briefly, the measurement of neurological deficit scores was tested as follows: 0: no deficit; 1: forelimb weakness and torso turning to the ipsilateral side when held by the tail; 2: circling to the affected side when held by the tail on the bench; 3: unable to bear weight on the affected side or spontaneous circling to the affected side; 4: no spontaneous locomotor activity or barrel rolling.

Immunofluorescence

After perfusion with PBS and 4% paraformaldehyde for 3 min, brain tissues were removed and placed into 4% paraformaldehyde at 4°C. After 24 h, brain tissue was dehydrated using 40% sucrose for 5 days, embedded in OTC, and frozen at −70°C. Brain tissues were sectioned into slices of 10 μm thickness with a cryotome (Leica, Mannheim, Germany) and then placed on adhesion microscope slides (Citoglas, China). Brain sections were fixed in 4% paraformaldehyde, permeabilized with 0.3% Triton X-100 in PBS, blocked with 5% normal donkey serum, and incubated overnight at 4°C with specific primary antibodies against cleaved-caspase-3, ROCK1, p-MLC, NenN, F-actin and NMMHC IIA (diluted at 1:100, Abcam, UK). Then, sections were incubated with corresponding secondary antibodies or Alexa Fluor® 568 phalloidin (diluted at 1:100, Thermo Fisher Scientific, USA) at room temperature. Fluorescent images were observed under confocal laser scanning microscopy. Quantitative co-localization of NMMHC IIA with F-actin was performed using the ImageJ software which can provide the Manders' coefficients for the overlap of the images.

Haematoxylin and Eosin (HE) Staining

Histomorphological analysis was performed by HE staining. Briefly, brain slices were put into haematoxylin and eosin solution, redehydrated in gradient ethanol solution again, treated with dimethylbenzene and covered with coverslips. A digital pathological section scanner (Hamamatsu, Japan) was used to screen pathological images and NDPView2 software analysed these images.

Western Blot Analysis

The tissues corresponding to the peri-ischemic cortex were taken out and then homogenized in the RIPA lysis buffer containing 1 mM PMSF. After centrifuging at 12,000 rpm for 10 min at 4°C, a bicinchoninic acid (BCA) protein assay kit (Bi yuntian Biotech. Co., Ltd., China) was used to determine the protein concentration of the supernatant. The supernatant was diluted by loading buffer to 1 μg/μL and then heated at 100°C for 5 min. Proteins (20 μg/well) were separated by SDA-PAGE and transferred to a PVDF membrane. The membranes were blocked for 2 h at room temperature in TBST containing 5% BSA, and then, it was incubated with specific primary antibodies overnight at 4°C: anti-bax, anti-bcl-2, anti-caspase 3, anti-ROCK1, anti-MLC, anti-p-MLC, anti-F-actin and anti-NMMHC IIA (diluted at 1:1000, Abcam, UK). After the membrane was washed with TBST, it was incubated for 2 h with a secondary antibody (goat anti-rabbit 1:10,000 Biomorld Technology, USA). Images were detected with ECL and imaged using the Gel Imaging System (BioRad, Hercules, CA, USA). Each experiment was performed with three independent replicates.

Co-Immunoprecipitation (Co-IP)

Briefly, 30 μL Protein A/G PLUS-Agarose was washed with RIPA buffer three times, and 2 μg antibodies were added to the agarose solution and incubated at 4°C overnight on a rotator. The prepared antibody-agarose complex was added to 1 mL of whole cell lysate (1 μg/μL) and incubated for 6 h at 4°C, followed by washing three times with RIPA buffer, adding 2×SDS gel loading buffer and boiling for 5 min. Proteins were detected by Western blot analysis.

Statistical Analysis

All data are expressed as the means±SD from at least three independent experiments. Data were analysed by Student's *t* test for two group comparisons or one-way analysis of variance (ANOVA), followed by Dunnett's post hoc test for multiple comparisons, using Graph Pad Prism 6.0 (Graph Pad Software, La Jolla, CA, USA). Differences were considered significant with a *P*-value less than 0.05.

Results

AAV-shMyh9 Delivered the Transgene Widely in the Brain

To deliver an AAV vector from circulating blood to the brain, we employed tail vein injection, because this provides a direct route to the brain. The transfection of AAV-GFP vehicle four weeks after the injection was observed under the fluorescence microscope by detecting the GFP-positive cells. The observation showed that the AAV vehicle was successfully transferred into nerve cells in the brain cortex (Figure 1).

AAV Mediates NMMHC IIA Inhibition in the Ischemic Area After the MCAO/R

To ensure the interference efficiency of AAV-shMyh9, we analyzed the expression of NMMHC IIA by Western blot and immunofluorescence four weeks after the injection. As expected, NMMHC IIA positive neurons (NMMHC IIA/NeuN positive cells) decreased on the NMMHC IIA shRNA-injected brain compared with the control shRNA-injected brain (Figure 2A and B). Western blot analysis revealed the similar results in NMMHC IIA expression (Figure 2C).

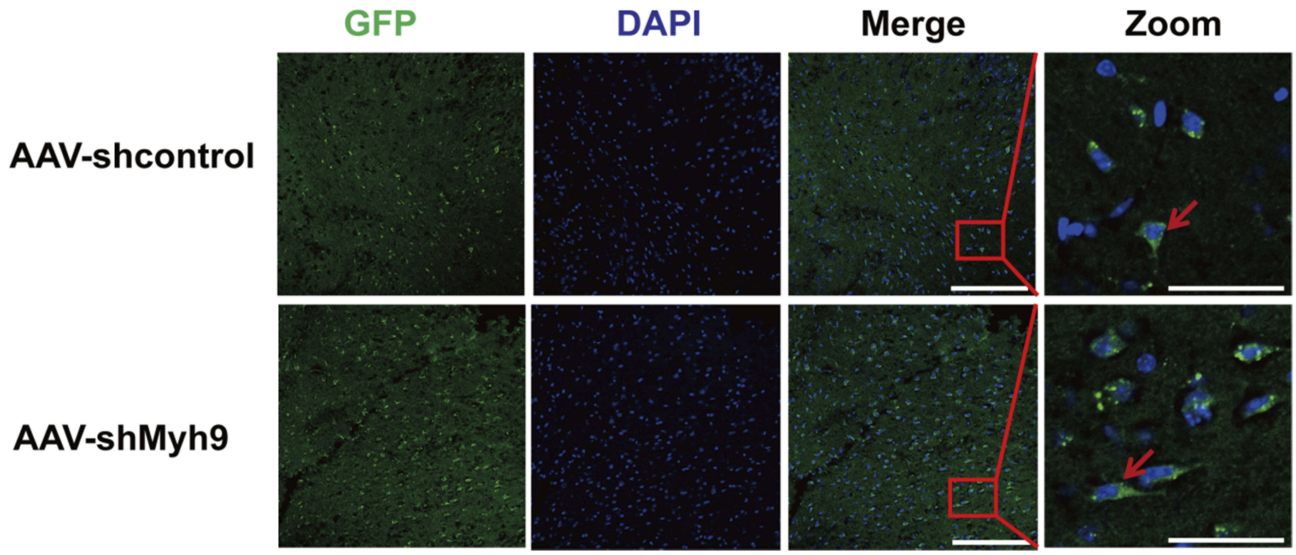

Figure 1 Confocal photomicrographs of GFP expression 4 weeks following injection of AAV-shMyh9. Brain sections from C57BL/6J mice 4 weeks after intravenous injection of AAV9-control-GFP or AAV9-sh NMMHC IIA-GFP (1.5×10^{11} genome copies/mouse). Bar: 50 μm. The red arrows indicate GFP-positive cells.

Because AAV-shMyh9-GFP (#3) showed the strongest interference efficiency, it was used for subsequent experiments.

NMMHC IIA Inhibition via the AAV Vector Improves Cerebral Ischemia-Reperfusion Injury After MCAO/R

To evaluate the neuroprotective effect of NMMHC IIA inhibition, AAV-shMyh9 or AAV-shcontrol was injected four weeks before MCAO/R attack. Twenty-four hours after reperfusion, neurological deficit scores were measured, and then the mice were killed for HE staining. The results showed that pretreatment with AAV9-shMyh9 significantly improved the neurological deficit compared with I/R group (Figure 3A). In I/R group, HE staining showed a large number of shrunken neurons with pyknotic nuclei (yellow arrow), which indicated dead neurons (Figure 3C). Notably, the abundance of dead neurons decreased and there were many intact neurons (blue arrow) in the AAV-shMyh9 group (Figure 3C). Statistical results showed that the intact neurons were 48.58±7.48% in I/R group. By contrast, AAV-shMyh9 treatment increased the intact neurons to 76.89±4.09% (Figure 3B).

NMMHC IIA Inhibition Reduced Apoptosis in the Ischemic Cortex Tissues After MCAO/R

Next, we examined whether the protective effect of NMMHC IIA inhibition is associated with inhibition of neuronal apoptosis induced by I/R. Four weeks after the injection of AAV, the mice were treated with I/R, and apoptosis-related proteins Bcl-2 and Bax in ischemic brain tissue were assessed. Compared with the sham group, Bax protein levels in the I/R group was significantly higher, while Bcl-2 protein expression was significantly lower compared with sham group values. In contrast, compared with I/R group, AAV-shMyh9 pretreatment significantly decreased Bax protein amounts (Figure 4A), and increased Bcl-2 protein expression (Figure 4B). We also detected neuronal apoptosis in the ischemic penumbra areas using TUNEL analysis. As shown in Figure 4C and D, there were more apoptotic neurons (TUNEL/NeuN-positive cells) in I/R group compared with sham group. However, AAV-shMyh9 treatment significantly decreased I/R-induced neuronal apoptosis.

NMMHC IIA Inhibition Attenuates I/R-Induced NMMHC IIA-Actin Interaction in Mice

It has been reported that NMMHC IIA-actin interaction is required to initiate actomyosin contractility, which further facilitates cellular apoptosis.[12] We next investigated if AAV-shMyh9 attenuated NMMHC IIA-actin interaction induced by I/R. According to an immunofluorescence assay, we identified an increased interaction between NMMHC IIA and F-actin under ischemic attack when compared with that of the sham group. However, NMMHC IIA-actin interaction was inhibited by AAV-shMyh9 (Figure 5A). We next applied the Manders' overlap coefficients to statistically quantify the colocalization of NMMHC IIA and F-actin. Quantitative results revealed that the colocalization of the two proteins was more striking in I/R group (Manders' coefficient: 0.895±0.03) than that in sham group (Manders' coefficient: 0.575±0.104), while AAV-

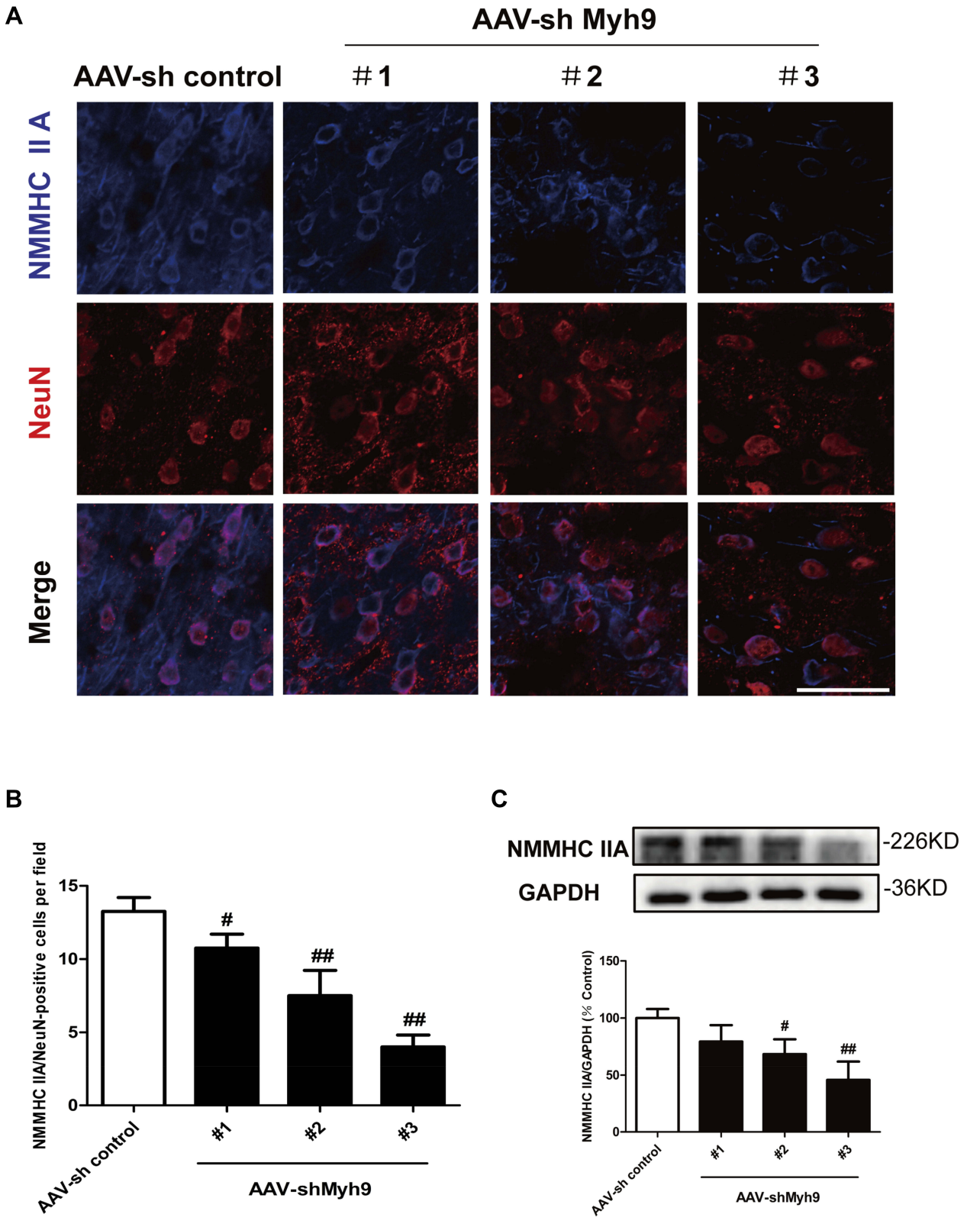

Figure 2 Efficacy of AAV-shMyh9 adenovirus transduction in vivo. 4 weeks after tail intravenous injection of AAV9-sh control-GFP or AAV9-shMyh9-GFP (#1, #2, #3), efficacy of AAV-shMyh9 adenovirus transduction were detected by immunofluorescence (**A, B**) and Western blot (**C**). Bar: 50 μm. The data are represented as means±SD of 3 individual experiments. $^{\#}P<0.05$ and $^{\#\#}P<0.01$ vs the AAV9-sh control group.

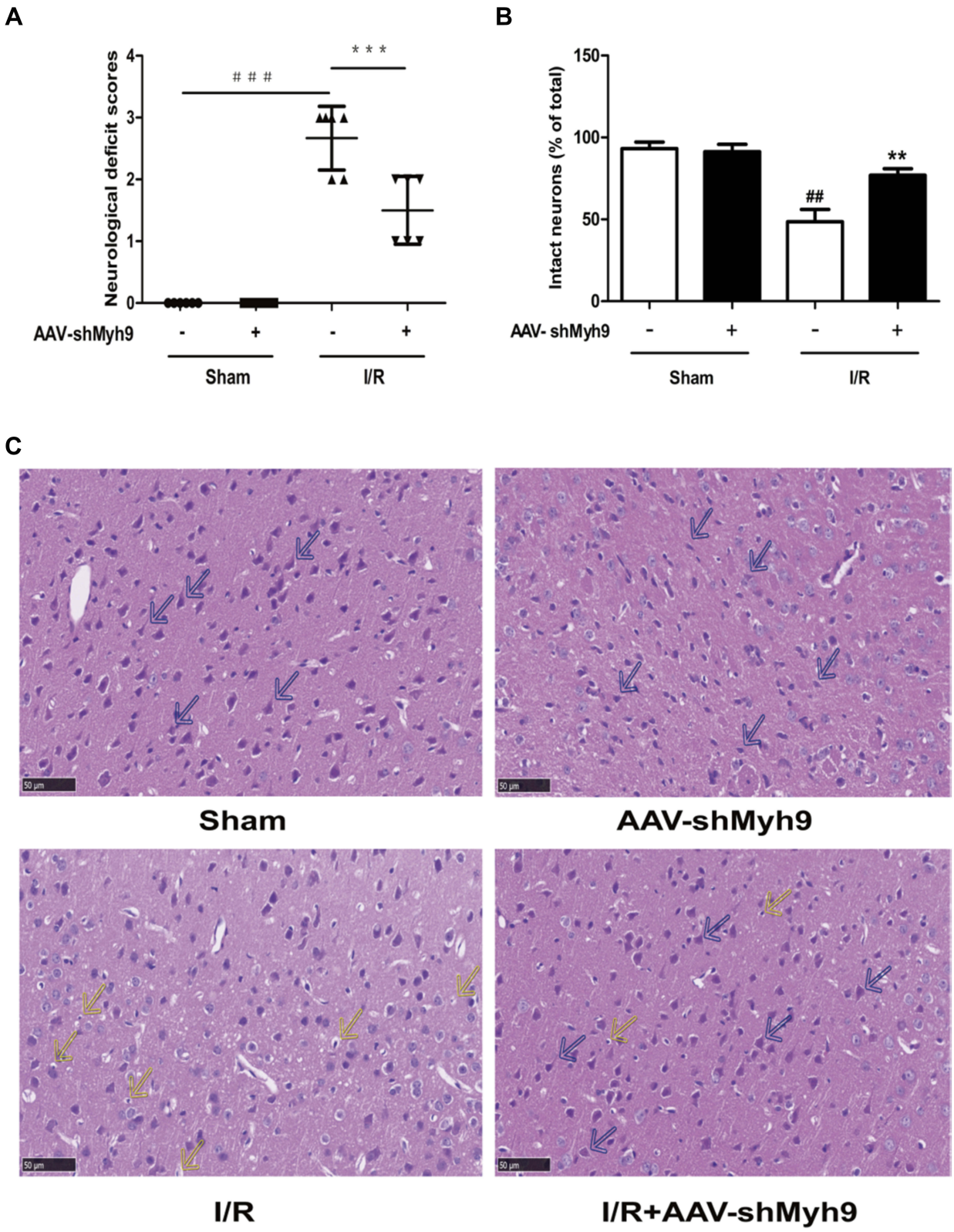

Figure 3 NMMHC IIA inhibition via the AAV vector improves cerebral ischemia-reperfusion injury after MCAO/R. (**A**) Neurological deficit scores in different groups. Results are expressed as the mean±SD, n=6. $^{\#\#\#}P<0.001$ vs sham group; $^{***}P<0.001$ vs model group. (**B**) Statistical analysis of intact neurons in the ischemic region. Results are expressed as the mean±SD, n=3. $^{\#\#}P<0.01$ vs sham group; $^{**}P<0.01$ vs model group. (**C**) HE staining showing the morphological characteristics of mouse brains upon MCAO/R. Shrunken neurons with pyknotic nuclei are indicated with yellow arrows while intact neurons are indicated with blue arrows. Bar: 50 μm.

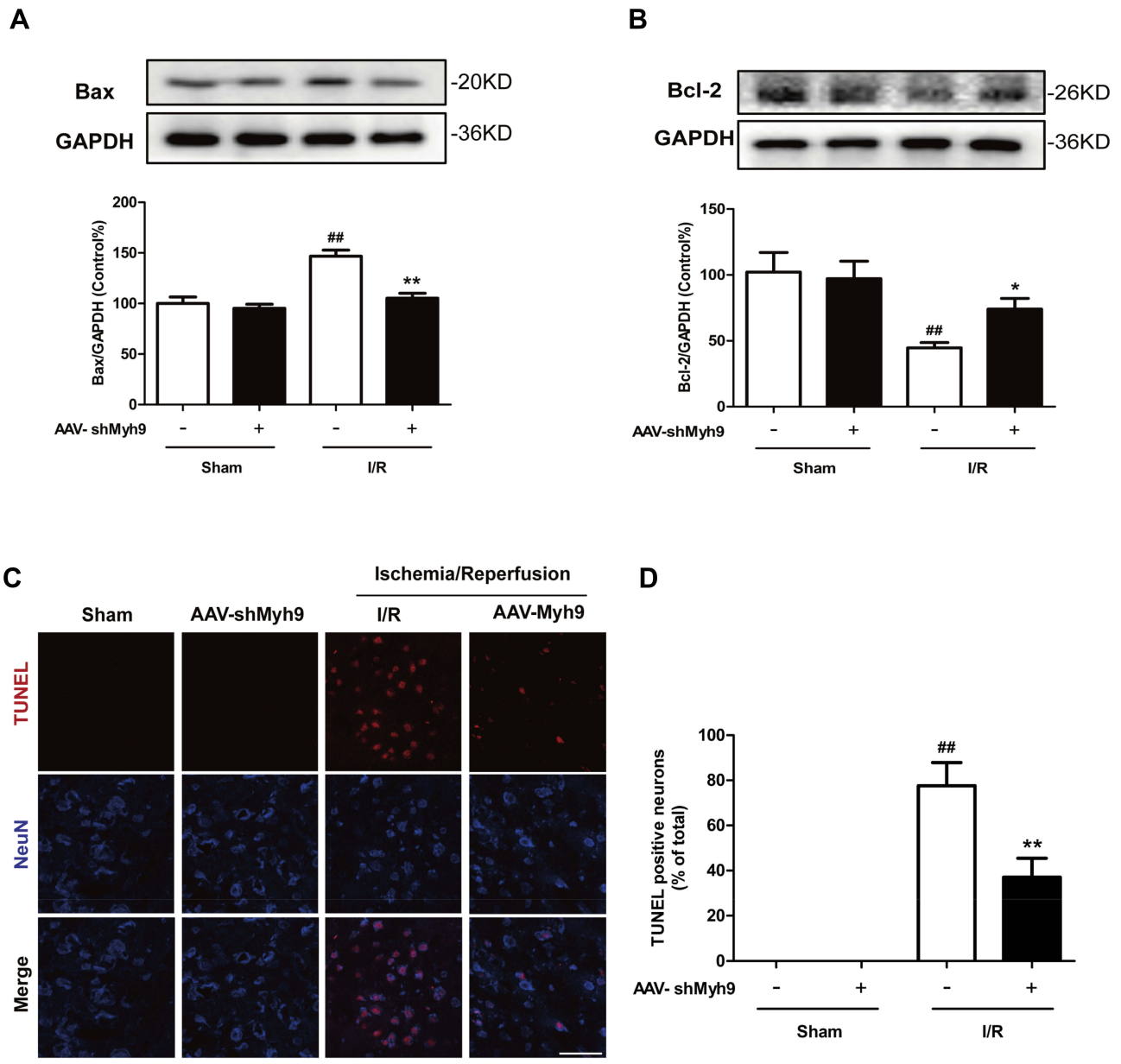

Figure 4 NMMHC IIA inhibition reduced apoptosis in the ischemic cortex tissues after MCAO/R. Immunoblots of Bax (**A**) and Bcl-2 (**B**) from total cell lysates of cortical tissue harvested 24 hrs after I/R. GAPDH was used as a control. (**C**) TUNEL analysis showing the apoptotic cells in penumbra of mouse brain upon MCAO. NeuN was stained to show neurons. Bar: 50 μm. (**D**) Quantitative assessment of TUNEL/NeuN-positive cells. All data are presented as the mean±SD of 3 independent experiments. $^{\#\#}P<0.01$ vs sham group; $^{*}P<0.05$ and $^{**}P<0.01$ vs I/R group.

shMyh9 significantly decreased the interaction of NMMHC IIA and F-actin (Manders' coefficient: 0.665±0.039) (Figure 5B). We further confirmed the interaction of NMMHC IIA and F-actin by Co-IP analysis. The results of immunoblotting analysis using anti-NMMHC IIA antibody demonstrated that I/R treatment enhanced the association of NMMHC IIA with F-actin, which was attenuated by AAV-shMyh9 pretreatment (Figure 5C). The statistical analysis also revealed that anti-F-actin antibody precipitated less NMMHC IIA protein in AAV-shMyh9-treated group, compared with I/R group (Figure 5D).

NMMHC IIA Inhibition Attenuates I/R-Induced Caspase 3/ROCK/MLC Pathway Activation

Studies have also shown that Caspase 3/ROCK/MLC pathway may be necessary for cytoskeletal reorganization and cell apoptosis. We consequently investigated the effect of AAV-shMyh9 on cytoskeleton-related caspases-3/ROCK1/MLC pathway. I/R caused a modest decrease in ROCK1 (Figure 6B) expression compared to the control, with increased levels of MLC phosphorylation

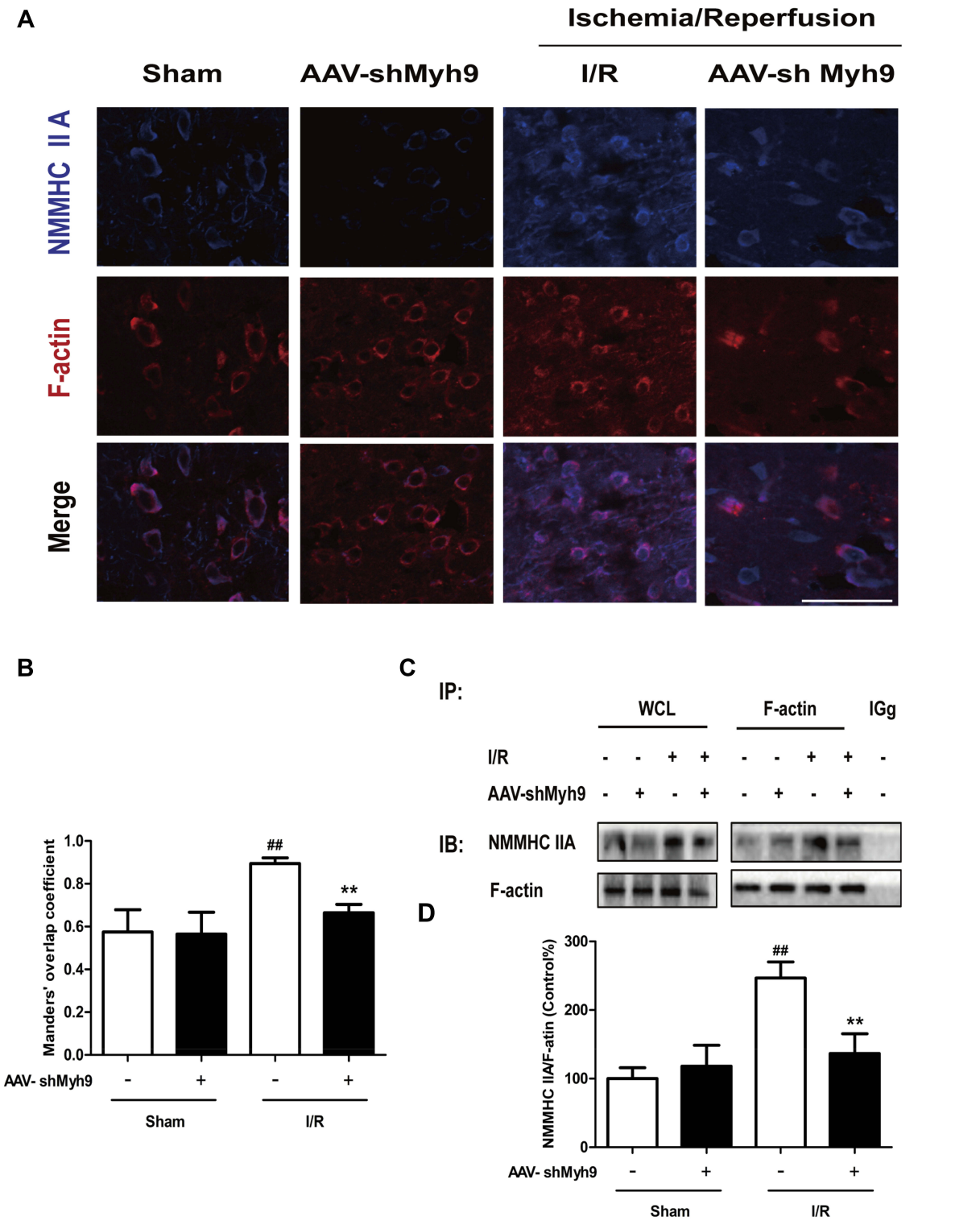

Figure 5 NMMHC IIA inhibition attenuates I/R-induced NMMHC IIA-actin interaction in mice. (**A**) Representative images of each group were shown. Mice in each group were sacrificed 24 hrs after the MCAO/R. Confocal microscopy was used to detect the expression of NMMHC IIA (blue) and F-actin (red). Bar: 50 μm. (**B**) The quantitative colocalization of NMMHC IIA with F-actin was evaluated on the basis of Manders' overlap coefficients. (**C**) Co-IP of NMMHC IIA and F-actin was detected by Western blots with indicated antibodies. The bands of left panel are from whole-cell lysates (WCL) and the bands of right panel are the same as shown on the left but immunoprecipitated with indicated antibodies. After MCAO/R, ischemic brain tissue lysates were subjected to immunoprecipitation with anti-F-actin antibody, and then the precipitates were analyzed by immunoblotting with anti-myosin IIA and anti-F-actin antibodies. Normal IgG was loaded as positive and negative controls. (**D**) Quantification of NMMHC IIA co-immunoprecipitated with F-actin in mice. Results were expressed as mean±SD from three independent experiments. $^{\#\#}P< 0.01$ versus sham group, $^{**}P< 0.01$ versus I/R group.

Abbreviations: IB, immunoblotting; IP, immunoprecipitation; IgG, immunoglobulin G.

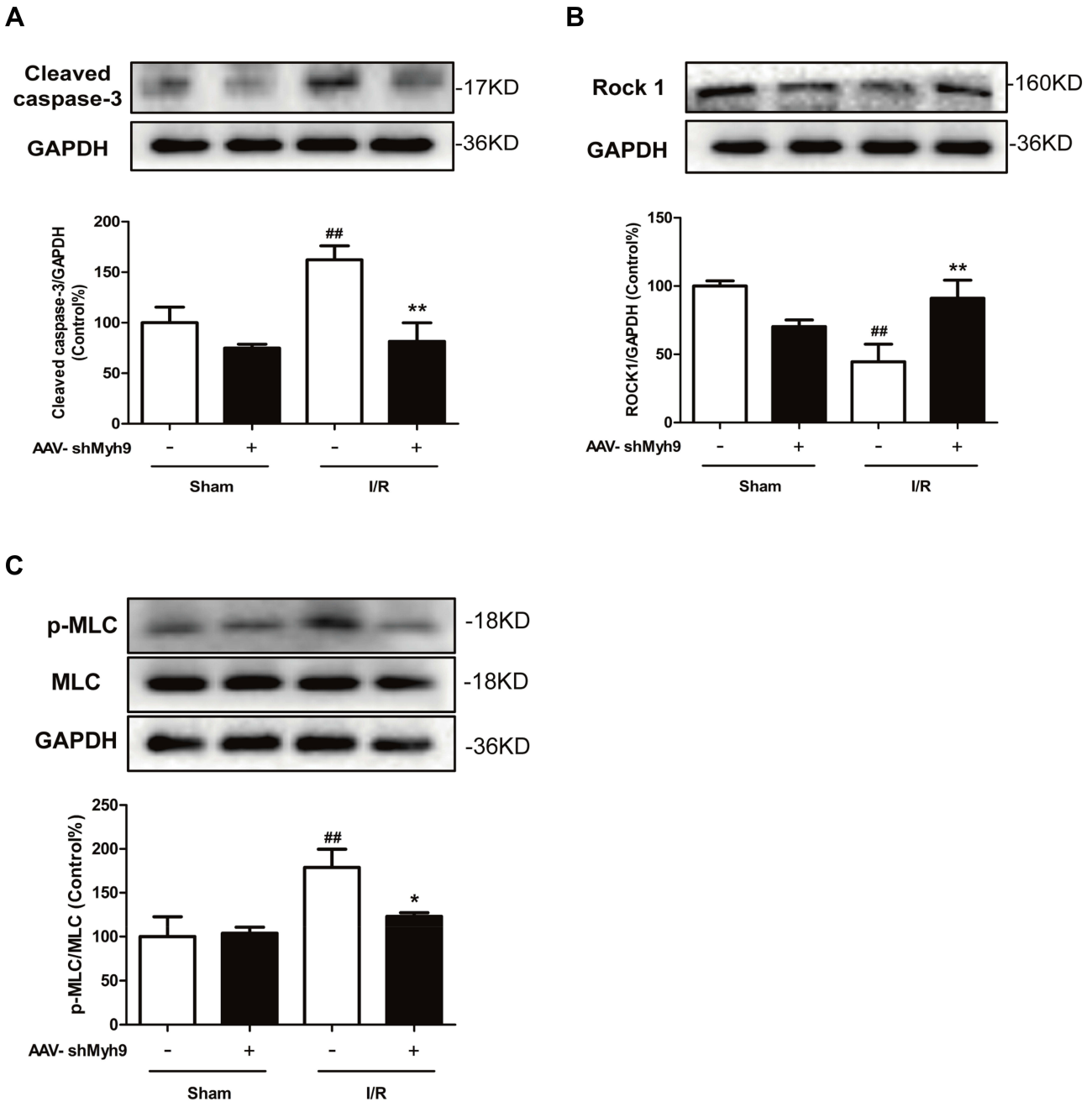

Figure 6 NMMHC IIA inhibition attenuates I/R-induced Caspase 3/ROCK/MLC pathway activation. Mice in each group were sacrificed 24 hrs after the MCAO/R. Tissue lysates were then subjected to Western blotting assay. Protein expression of cleaved-caspase 3 (**A**), ROCK1 (**B**) and phosphorylated MLC/MLC (**C**) were measured using relevant antibodies. All data are presented as the mean±SD of 3 independent experiments. $^{\#\#}P<0.01$ vs sham group; $^{*}P<0.01$ and $^{**}P<0.01$ vs I/R group.

(Figure 6C) and cleaved caspase-3 (Figure 6A). However, compared with I/R group, pretreatment with AAV-shMyh9 elevated ROCK1 expression (Figure 6B), while it blocked caspase-3 cleavage (Figure 6A) and reduced levels of phosphor-MLC (Figure 6C). The expressions of activated caspase-3, ROCK1 and p-MLC in neurons were further investigated by double immunostaining in ischemic brain after I/R. Antibody against neuronal nuclei (NeuN) was used to identify neurons. Immunofluorescence analysis demonstrated that I/R caused an increased cleaved caspase-3 and p-MLC immunoreactivity in neurons compared to the sham group. AAV-shMyh9 pretreatment inhibited the up-regulated cleaved caspase-3 (Figure 7A and D), MLC phosphorylation (Figure 7C and D) and down-regulated ROCK1 (Figure 7B and D) in neurons induced by I/R.

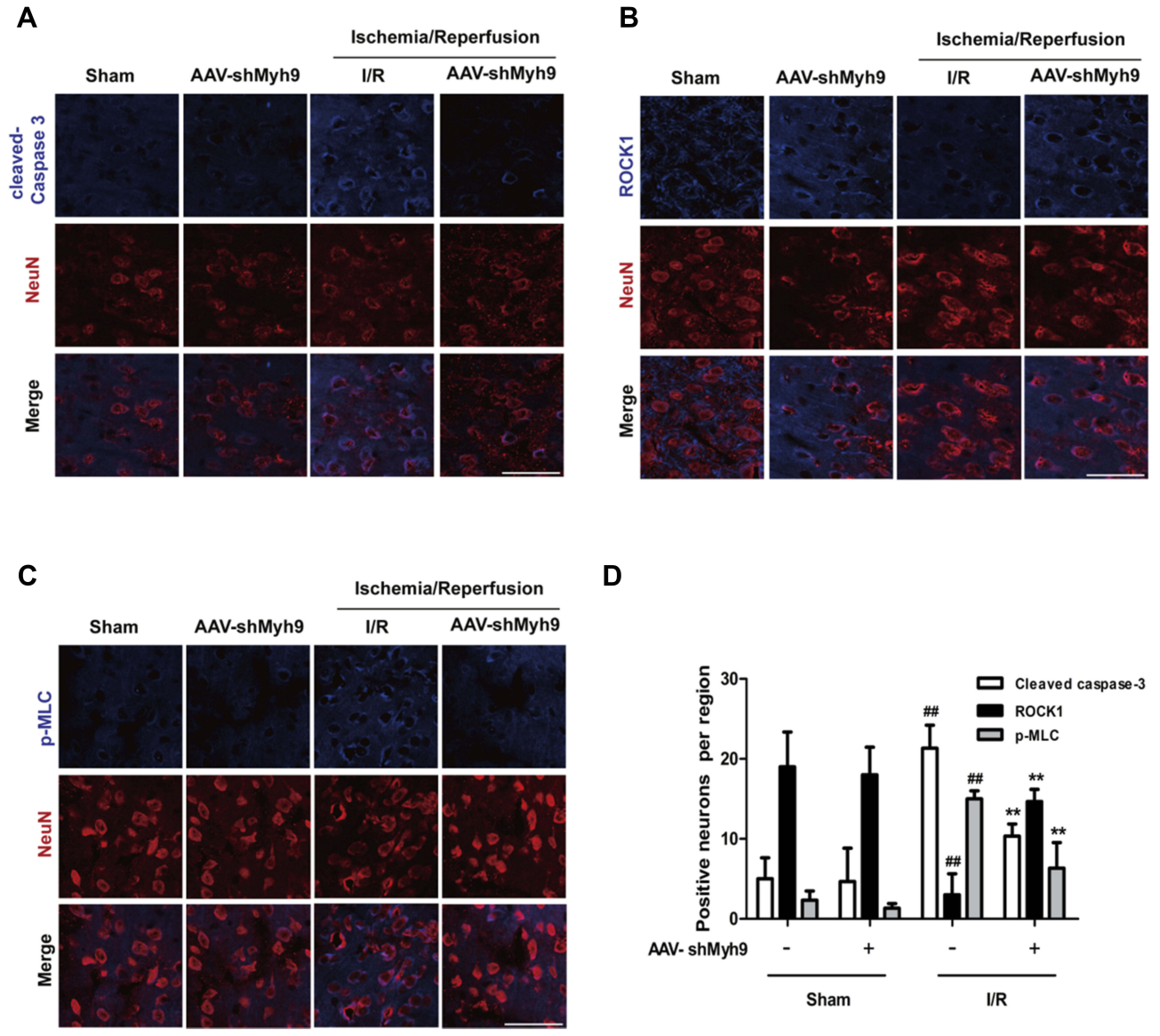

Figure 7 NMMHC IIA inhibition attenuates I/R-induced caspase-3/ROCK1/MLC activation in neurons. Mice in each group were sacrificed 24 hrs after the MCAO/R. Tissue sections were then subjected to immunofluorescence. Then, confocal microscope was used to detect cleaved caspase-3 (**A**), ROCK1 (**B**), p-MLC (**C**, blue) and Neun (red). Bar: 50 μm. (**D**) Quantitative assessment of the numbers of cleaved caspase-3, ROCK1 and p-MLC positive neurons in sham and MCAO group. Results are expressed as the mean±SD, n=3. $^{\#\#}P<0.01$ vs sham group; $^{**}P<0.01$ vs I/R group.

Discussion

RNA interference is an evolutionarily conserved process that can silence specific genes through double-stranded RNA.[24] In mammalian cells, viral vectors have been widely used to effectively transfer siRNA and shRNA.[25,26] Recombinant AAV (rAAV) system is one of the most reliable carriers for gene delivery to the CNS. Many reasons make AAV system an ideal gene delivery tool for the CNS. For example, AAV showed a strong preference for neuronal infection, no pathogenicity, and a single delivery could achieve lasting expression.[20] Among more than one hundred AAVs, we finally choose AAV9 as a virus vector to infect mice. Because AAV9 could easily cross the BBB, and has a high gene transduction efficiency in neurons after intravenous injection in neonatal mice.[27] Herein, we observed widespread expression of GFP in the brain 4 weeks following AAV administration (Figure 1). The results are consistent with previous studies.[28] Western analysis revealed that cortex from shMyh9 animals exhibited a significant reduction in NMMHC IIA expression, indicative of specific RNAi targeting (Figure 2). In the present study, AAV-mediated gene delivery before the ischemic period has been used to assess the effect of NMMHC IIA in cerebral ischemia.

Actin motor protein NMMHC IIA, as an important regulator of cell morphology, plays an indispensable role in a series of cell processes, such as cell migration, cell adhesion and so on.[29] In addition to its roles in normal cellular physiological processes, NMMHC IIA has recently been reported to be involved in many diseases, including neuronal disorders, cancer and cardiovascular diseases.[30,31] In addition, increasing evidences have indicated that NMMHC IIA is involved in the pathogenic process of ischemia stroke. Clinical reports showed that a patient with Myh9 gene mutation experienced ischemic stroke.[32] Additionally, NMMHC IIA also has been identified to participate in BBB dysfunction in ischemia stroke, and the NMMHC IIA-actin interaction mediates H_2O_2-induced neuronal apoptosis.[8,12] NMMHC IIA is also an attractive therapeutic target in ischemic stroke. Zhao et al found that TRPM7 kinase modulates OGD/R-induced neuronal apoptosis via annexin 1 carried by NMMHC IIA, blocking NMMHC IIA function by its antagonist blebbistatin was found to improve learning and memory in rats after MCAO and could also improve cell viability after OGD/R.[33] However, application of blebbistatin requires extra caution because the compound has some serious side effects, including structural instability and cytotoxicity, which may mask possible myosin-specific effects. To overcome these hurdles, AAV vectors expressing shRNAs targeting the mouse Myh9 gene was developed. In our study, AAV-shMyh9 significantly improved neurological scores (Figure 3A) and histological injury (Figure 3B and C) after MCAO/R.

Previous studies have confirmed that neuronal apoptosis is one of the pathological mechanisms of ischemic stroke, and preventing neuronal apoptosis will be an effective treatment for this terrible disease.[34] After ischemic stroke, mitochondrial apoptotic pathway played a key role in regulating neuronal apoptosis.[35] The release of mitochondrial CytC leads to the activation of caspase-3, which eventually induce neuronal apoptosis. Furthermore, Bcl-2 regulates apoptosis by altering mitochondrial permeability and CytC release. When death signals are received, pro-apoptotic protein Bax promotes the release of CytC from mitochondria to cytoplasm, whereas anti-apoptotic protein Bcl-xl inhibits this process.[36] According to our study, AAV-shMyh9 inhibits neuronal apoptosis in MCAO/R mice including down-regulating Bax (Figure 4A), cleaved caspase-3 (Figure 6A) and up-regulating Bcl-2 levels (Figure 4B), further confirming the protective effect of AAV-shMyh9 in ischemic stroke.

Studies have shown that the interaction of NMMHC II with actin filaments in generating forces during the execution phase of apoptosis.[37] When under injury, F-actin is reported to polymerize at the distal end of injured neuritis and undergoes reorganization and retrograde flow generated by the actin-binding motor protein, NMMHC II.[38,39] Our previous studies have confirmed that morphological changes in apoptotic cells are dependent on actomyosin cytoskeleton remodeling in H_2O_2-treated neurons.[12] When neurons are stimulated by H_2O_2, the interaction between NMMHC IIA and F-actin increased, which provided a basis for generating contractile forces, and ultimately leading to membrane blebbing and neuronal apoptosis. However, little is known about the specific function of NMMHC IIA in neuronal apoptosis under ischemic attack. In this study, pretreatment with AAV-shMyh9 attenuated I/R-induced NMMHC IIA-actin interaction and the subsequent neuronal apoptosis. This result is consistent with the Co-IP analysis, which reflects the amount of NMMHC IIA overlapping with actin (Figure 5).

Furthermore, MLC phosphorylation increases contractility of the actomyosin system, which leads to dynamic membrane blebbing and subsequent cell apoptosis. The phosphorylation of MLC is the result of the cleavage of a Rho GTPase effector, the kinase ROCK1, by caspase-3. This cleavage induces a constitutive kinase activity by removing the inhibitory domain.[37] Moreover, caspase-3/ROCK1/MLC has also been proved to be a novel cyclic positive feedback loop for regulating apoptosis in different cell types, such as cardiac myocyte, human leukemia cells and neurons.[40–42] We have previously reported the caspase-3/ROCK1/MLC feedback loop in H_2O_2-induced PC12 cell injury, and NMMHC IIA is also involved in a positive feedback loop that links caspase-3/ROCK1/MLC signaling axis.[13,22] Our present findings confirmed that I/R-induced caspase-3 cleavage led to decrease of ROCK1 and MLC phosphorylation. Pretreatment with AAV-shMyh9 inhibited the activation of caspase-3, ROCK1 and MLC, reorganized the subsequent NMMHC IIA-actin cytoskeletal system, and ultimately protected against I/R-induced neuronal apoptosis (Figures 6 and 7). These findings provide the first evidence that Caspase-3/ROCK1/MLC/NMMHC IIA-actin positive feedback loop is involved in neuronal apoptosis induced by I/R.

In conclusion, we have demonstrated that AAV-based neuron-specific gene delivery system can perform functional gene expression in mouse brain. NMMHC IIA inhibition with AAV-shMyh9 has the potential for amelioration of ischemic damage via an anti-apoptotic mechanism. The potential mechanism of NMMHC IIA inhibition is related to inhibit NMMHC IIA-actin interaction and caspase-3/ROCK1/MLC signaling pathway (Figure 8). This study is the first to reveal the correlation between NMMHC IIA and the caspase-3/ROCK1/MLC positive feedback loop in

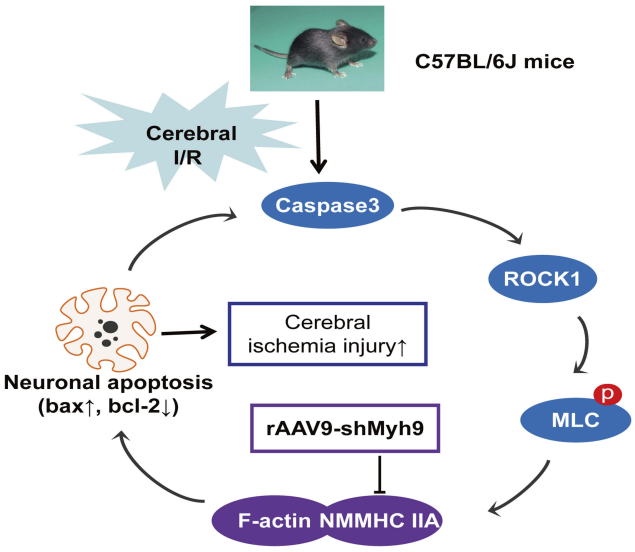

Figure 8 Schematic overview of the proposed mechanism for AAV9-shMyh9 against I/R-induced neuronal injury. I/R induces caspase-3 cleavage, the activation of ROCK1, and then the phosphorylation of MLC (Ser-19), which activates NMMHC IIA and facilitates its association with actin, initiating cell apoptosis. The increased NMMHC IIA-actin interaction, in turn, amplifies the activation of caspase-3, sensitizing I/R-induced apoptosis. AAV9-shMyh9 could directly interfere with the NMMHC IIA-actin interaction, and then inhibit caspase3/ROCK1/MLC signaling pathway activation, attenuate apoptotic under I/R.

ischemic stroke and also provides further evidence for its potential value in the cerebral ischemia therapy.

Acknowledgments

This research work was supported by The Funding of Double First-rate Discipline Innovation Team (CPU2018GF07) and Postgraduate Research & Practice Innovation Program of Jiangsu Province (Grants No. KYCX17_0668).

Disclosure

The authors declare no conflicts of interest in this work.

References

1. Chen N, Zhou Z, Li J, et al. 3-n-butylphthalide exerts neuroprotective effects by enhancing anti-oxidation and attenuating mitochondrial dysfunction in an in vitro model of ischemic stroke. *Drug Des Devel Ther*. 2018;12:4261–4271. doi:10.2147/DDDT.S189472
2. Pandian JD, Gall SL, Kate MP, et al. Prevention of stroke: a global perspective. *Lancet*. 2018;392(10154):1269–1278. doi:10.1016/S0140-6736(18)31269-8
3. Ozaki T, Nakamura H, Kishima H. Therapeutic strategy against ischemic stroke with the concept of neurovascular unit. *Neurochem Int*. 2019;126:246–251. doi:10.1016/j.neuint.2019.03.022
4. Siniscalchi A, De Sarro G, Pacifici R, Pisani E, Sanguigni S, Gallelli L. Thrombolytic therapy in cocaine users with ischemic stroke: a review of current practice. *Psychopharmacol Bull*. 2019;49(1):70–79.
5. Puyal J, Ginet V, Clarke PG. Multiple interacting cell death mechanisms in the mediation of excitotoxicity and ischemic brain damage: a challenge for neuroprotection. *Prog Neurobiol*. 2013;105:24–48. doi:10.1016/j.pneurobio.2013.03.002
6. Li X, Zheng L, Xia Q, et al. A novel cell-penetrating peptide protects against neuron apoptosis after cerebral ischemia by inhibiting the nuclear translocation of annexin A1. *Cell Death Differ*. 2018;26(2):260–275. doi:10.1038/s41418-018-0116-5
7. Zhang YP, Zhang Y, Xiao ZB, et al. CFTR prevents neuronal apoptosis following cerebral ischemia reperfusion via regulating mitochondrial oxidative stress. *J Mol Med (Berl)*. 2018;96(7):611–620. doi:10.1007/s00109-018-1649-2
8. Lee JC, Won MH. Neuroprotection of antioxidant enzymes against transient global cerebral ischemia in gerbils. *Anat Cell Biol*. 2014;47(3):149–156. doi:10.5115/acb.2014.47.3.149
9. Coleman ML, Sahai EA, Yeo M, Bosch M, Dewar A, Olson MF. Membrane blebbing during apoptosis results from caspase-mediated activation of ROCK I. *Nat Cell Biol*. 2001;3(4):339. doi:10.1038/35070009
10. Sebbagh M, Renvoizé C, Hamelin J, Riché N, Bertoglio J, Bréard J. Caspase-3-mediated cleavage of ROCK I induces MLC phosphorylation and apoptotic membrane blebbing. *Nat Cell Biol*. 2001;3(4):346. doi:10.1038/35070019
11. Shen K, Wang Y, Zhang Y, et al. Cocktail of four active components derived from Sheng Mai San inhibits hydrogen peroxide-induced PC12 cell apoptosis linked with the caspase-3/ROCK1/MLC pathway. *Rejuvenation Res*. 2015;18(6):517–527. doi:10.1089/rej.2015.1697
12. Wang Y, Xu Y, Liu Q, et al. Myosin IIA-related actomyosin contractility mediates oxidative stress-induced neuronal apoptosis. *Front Mol Neurosci*. 2017;10:75. doi:10.3389/fnmol.2017.00075
13. Titus MA. Growing, splitting and stacking myosin II filaments. *Nat Cell Biol*. 2017;19(2):77. doi:10.1038/ncb3468
14. Hu S, Dasbiswas K, Guo Z, et al. Long-range self-organization of cytoskeletal myosin II filament stacks. *Nat Cell Biol*. 2017;19(2):133. doi:10.1038/ncb3466
15. Meddens MB, Pandzic E, Slotman JA, et al. Actomyosin-dependent dynamic spatial patterns of cytoskeletal components drive mesoscale podosome organization. *Nat Commun*. 2016;7:13127. doi:10.1038/ncomms13127
16. Lv Y, Fu L. The potential mechanism for Hydroxysafflor yellow A attenuating blood-brain barrier dysfunction via tight junction signaling pathways excavated by an integrated serial affinity chromatography and shotgun proteomics analysis approach. *Neurochem Int*. 2018;112:38–48. doi:10.1016/j.neuint.2017.10.012

17. Naso MF, Tomkowicz B, Perry WL, Strohl WR. Adeno-associated virus (AAV) as a vector for gene therapy. *BioDrugs*. 2017;31(4):317–334. doi:10.1007/s40259-017-0234-5
18. Qu Y, Liu Y, Noor AF, Tran J, Li R. Characteristics and advantages of adeno-associated virus vector-mediated gene therapy for neurodegenerative diseases. *Neural Regen Res*. 2019;14(6):931. doi:10.4103/1673-5374.250570
19. Wang D, Tai PWL, Gao G. Adeno-associated virus vector as a platform for gene therapy delivery. *Nat Rev Drug Discov*. 2019;18(5):358–378. doi:10.1038/s41573-019-0012-9
20. Weinberg MS, Samulski RJ, McCown TJ. Adeno-associated virus (AAV) gene therapy for neurological disease. *Neuropharmacology*. 2013;69:82–88. doi:10.1016/j.neuropharm.2012.03.004
21. Zeng J, Wang Y, Luo Z, et al. TRIM9-mediated resolution of neuroinflammation confers neuroprotection upon ischemic stroke in mice. *Cell Rep*. 2019;27(2):549–560. e6. doi:10.1016/j.celrep.2018.12.055
22. Sehara Y, Inaba T, Urabe T, et al. Survivin overexpression via adeno-associated virus vector Rh10 ameliorates ischemic damage after middle cerebral artery occlusion in rats. *Eur J Neurosci*. 2018;48(12):3466–3476. doi:10.1111/ejn.2018.48.issue-12
23. Cao G, Jiang N, Hu Y, et al. Ruscogenin attenuates cerebral ischemia-induced blood-brain barrier dysfunction by suppressing TXNIP/NLRP3 inflammasome activation and the MAPK pathway. *Int J Mol Sci*. 2016;17(9):1418. doi:10.3390/ijms17091418
24. Vélez AM, Fishilevich E. The mysteries of insect RNAi: a focus on dsRNA uptake and transport. *Pestic Biochem Physiol*. 2018;151:25–31. doi:10.1016/j.pestbp.2018.08.005
25. Schuster S, Miesen P, van Rij RP. Antiviral RNAi in insects and mammals: parallels and differences. *Viruses*. 2019;11:(5)448. doi:10.3390/v11050448
26. Weng Y, Xiao H, Zhang J, Liang XJ, Huang Y. RNAi therapeutic and its innovative biotechnological evolution. *Biotechnol Adv*. 2019;37(5):801–825. doi:10.1016/j.biotechadv.2019.04.012
27. Foust KD, Nurre E, Montgomery CL, Hernandez A, Chan CM, Kaspar BK. Intravascular AAV9 preferentially targets neonatal neurons and adult astrocytes. *Nat Biotechnol*. 2009;27(1):59–65. doi:10.1038/nbt.1515
28. Guo YY, Lu Y, Zheng Y, et al. Ubiquitin c-terminal hydrolase l1 (uch-l1) promotes hippocampus-dependent memory via its deubiquitinating effect on trkb. *J Neurosci*. 2017;37(25):5978–5995. doi:10.1523/JNEUROSCI.3148-16.2017
29. Xiao Q, Hu X, Wei Z, Tam KY. Cytoskeleton molecular motors: structures and their functions in neuron. *Int J Biol Sci*. 2016;12(9):1083–1092. doi:10.7150/ijbs.15633
30. Newell-Litwa KA, Horwitz R, Lamers ML. Non-muscle myosin II in disease: mechanisms and therapeutic opportunities. *Dis Model Mech*. 2015;8(12):1495–1515. doi:10.1242/dmm.022103
31. Ma X, Adelstein RS. The role of vertebrate nonmuscle Myosin II in development and human disease. *Bioarchitecture*. 2014;4(3):88–102. doi:10.4161/bioa.29766
32. Nishiyama Y, Akaishi J, Katsumata T, Katsura K, Katayama Y. Cerebral infarction in a patient with macrothrombocytopenia with leukocyte inclusions (MTCP, May-Hegglin anomaly/Sebastian syndrome). *J Nippon Med Sch*. 2008;75(4):228–232. doi:10.1272/jnms.75.228
33. Zhao Y, Wang J, Jiang H, Yu Z, Li X, Shi J. Following OGD/R, annexin 1 nuclear translocation and subsequent induction of apoptosis in neurons are assisted by myosin IIA in a TRPM7 kinase-dependent manner. *Mol Neurobiol*. 2015;51(2):729–742. doi:10.1007/s12035-014-8781-y
34. Sekerdag E, Solaroglu I, Gursoy-Ozdemir Y. Cell death mechanisms in stroke and novel molecular and cellular treatment options. *Curr Neuropharmacol*. 2018;16(9):1396–1415. doi:10.2174/1570159X16666180302115544
35. Fricker M, Tolkovsky AM, Borutaite V, Coleman M, Brown GC. Neuronal cell death. *Physiol Rev*. 2018;98(2):813–880. doi:10.1152/physrev.00011.2017
36. Zhang X, Zhang Y, Tang S, et al. Pien-Tze-Huang protects cerebral ischemic injury by inhibiting neuronal apoptosis in acute ischemic stroke rats. *J Ethnopharmacol*. 2018;219:117–125. doi:10.1016/j.jep.2018.03.018
37. Ndozangue-Touriguine O, Hamelin J, Bréard J. Cytoskeleton and apoptosis. *Biochem Pharmacol*. 2008;76(1):11–18. doi:10.1016/j.bcp.2008.03.016
38. Yu P, Santiago LY, Katagiri Y, Geller HM. Myosin II activity regulates neurite outgrowth and guidance in response to chondroitin sulfate proteoglycans. *J Neurochem*. 2012;120(6):1117–1128. doi:10.1111/j.1471-4159.2011.07638.x
39. Medeiros NA, Burnette DT, Forscher FP. Myosin II functions in actin-bundle turnover in neuronal growth cones. *Nat Cell Biol*. 2006;8(3):216. doi:10.1038/ncb1367
40. Chang J, Xie M, Shah VR, et al. Activation of Rho-associated coiled-coil protein kinase 1 (ROCK-1) by caspase-3 cleavage plays an essential role in cardiac myocyte apoptosis. *Proc Natl Acad Sci USA*. 2006;103(39):14495–14500. doi:10.1073/pnas.0601911103
41. Liu L, Li G, Li Q, et al. Triptolide induces apoptosis in human leukemia cells through caspase-3-mediated ROCK1 activation and MLC phosphorylation. *Cell Death Dis*. 2013;4:e941. doi:10.1038/cddis.2013.469
42. Wang Y, Liu Q, Xu Y, et al. Ginsenoside Rg1 protects against oxidative stress-induced neuronal apoptosis through myosin IIA-actin related cytoskeletal reorganization. *Int J Biol Sci*. 2016;12(11):1341. doi:10.7150/ijbs.15992